Science Discovery Chemistry
2026, Vol. 1, No. 1, pp. 41–51
https://doi.org/10.11648/j.sdc.20260101.15

Research Article

Synthesis of Copper–2,5-dimethylphenol –Cyclodextrin Nanomaterials and pH-Dependent of 2,5-dimethylphenol –Cyclodextrin Inclusion Complexes

Narayanasamy Rajendiran[1, *], Ayyadurai Mani[1], Palanichamy Ramasamy[2], Sengamalai Senthilmurugan[3]

[1]Department of Chemistry, Annamalai University, Annamalai Nagar, India
[2]Molecular Biophysics Unit, Indian Institute of Science, Bangalore, India
[3]Department of Zoology, Annamalai University, Annamalai Nagar, India

Abstract

Absorption, emission, and time-resolved fluorescence maxima of 2,5-dimethylphenol (25DMP) were examined in various solvents, as well as in α-CD and β-CD solutions at pH ~2, pH ~7, and pH ~11. The corresponding nanomaterials were synthesized and characterized using SEM, DSC, FTIR, XRD, and ^{1}H NMR analyses. At pH ~1 and pH ~7, the absorption/emission maxima and overall spectral profiles of 25DMP in α-CD and β-CD solutions were similar, but differed markedly at pH ~11, suggesting the presence of at least two distinct types of inclusion complexes. PM3 calculations indicate that 25DMP is more deeply embedded within the non-polar region of the β-CD cavity than in α-CD. Solvatochromic studies further show that the absorption and emission maxima of 25DMP display negligible shifts from cyclohexane to water. The fluorescence lifetimes of the 25DMP: CD complexes were greater than those of free 25DMP. The calculated HOMO–LUMO energy gap, total energy, free energy, enthalpy, entropy, dipole moment, and zero-point vibrational energy of the CD: 25DMPcomplex differed significantly from those of the isolated 25DMP, α-CD and β-CD molecules, and both the vertical and horizontal bond lengths between the methyl and hydroxy groups are smaller than the β-CD cavity size confirming the formation of an inclusion complex. SEM images along with DSC, FTIR, XRD, and ^{1}H NMR data reveal clear differences between Cu nanoparticles, free 25DMP, and the Cu: 25DMP: α-CD and Cu: 25DMP: β-CD nanomaterials. SEM-EDX analysis confirms the presence of 49.95% carbon, 44.03% oxygen, and 3.98% nano-Cu in the prepared nanomaterials.

Keywords

2,5-dimethylphenol, Cyclodextrin, Copper Nano, pH Effects

*Correspondence: Narayanasamy Rajendiran (drrajendiran1967@gmail.com)

Received: 11 March 2026; **Accepted:** 23 March 2026; **Published:** 10 April 2026

1. Introduction

It is well established that the photophysical and spectral properties of aromatic hydrocarbons are strongly influenced not only by the nature of their substituents but also by their position on the aromatic ring, particularly when multiple substituents are present [1-16]. For instance, substituted phenols, benzoic acids, diaminobenzenes, and diamino-naphthalene derivatives [17-20] exhibit distinct photophysical behaviors, and their responses to solvent polarity and hydrogen-bonding tendencies vary considerably. Consequently, these and similar molecules serve as excellent probes for characterizing macro- and biomolecular environments [21-30]. Another key property influenced by substituent position is acid–base behavior; it is now well recognized that the acidity and basicity of such functional groups undergo significant changes upon excitation to the S_1 state [31, 32].

In this context, we investigated the behavior of 2,5-dimethylphenol (25DMP) in the presence of α-CD and β-CD, which are widely used as model systems for studying cyclodextrin inclusion complexation. Owing to challenges in accurately modeling solvation effects, only gas-phase host–guest interactions were considered computationally. The interactions between 25DMP and the CDs were examined, and the experimental findings were compared with theoretical predictions. The present work focuses on: (i) absorption and fluorescence spectral shifts and the first excited singlet-state lifetimes of 25DMP in α-CD, β-CD, solvents of varying polarity, and different pH conditions; (ii) proton-transfer behavior of 25DMP in aqueous, α-CD, and β-CD media; (iii) the structures and geometries of the inclusion complexes using PM3 molecular modeling; and (iv) the effect of doping 25DMP: CD complexes on copper nanomaterials, analyzed through DSC, FTIR, ^{1}H NMR, and SEM techniques.

2. Materials and Methods

2.1. Preparation of CD Solution

The stock solution of 25DMP was prepared at a concentration of 2×10^{-2} mol/dm^3. Aliquots of 0.1 or 0.2 ml of this stock were transferred into 10 ml volumetric flasks. To each flask, varying concentrations of α-CD or β-CD (0.2, 0.4, 0.6, 0.8, and 1.0 × 10 mol/dm^3) were added. The mixtures were then diluted to 10 ml with triply distilled water and thoroughly shaken. The final concentration of 25DMP in all solutions was maintained at 4×10^{-4} mol/dm^3. All experiments were conducted at room temperature (298 K).

2.2. Synthesis of Cu: 25DMP: CD Nanomaterials

A 100 ml solution of $CuSO_4$ (1×10^{-3} mol/dm^3) in a round-bottom flask was reduced by the dropwise addition of 1% sodium borohydride while stirring vigorously on a hot plate with a magnetic stirrer. As the reaction proceeded, the solution color changed from pale blue to reddish brown. Subsequently, 5 ml of 1% trisodium citrate was added dropwise as a stabilizing agent.

Separately, α-CD or β-CD (1 mmol) was dissolved in 40 ml of distilled water, and 25DMP (1 mmol) dissolved in 10 ml ethanol was added slowly to the CD solution. The mixture was stirred at 50°C for 2 hours. The prepared copper nanoparticle solution was then added to this mixture and stirred for an additional 2 hours at 40–50°C. The resulting solution was freeze-dried using a mini-lyophilizer at –80°C to obtain a powdered product. The Cu: 25DMP: CD nanomaterial was washed with small amounts of ethanol and water to remove unreacted 25DMP, copper, and CD. The purified precipitate was dried under vacuum at room temperature and stored in an airtight container. The resulting Cu: 25DMP: CD powder samples were used for further characterization [33-37].

3. Results and Discussion

3.1. Effect of α-CD and β-CD on 2,5-dimethylphenol at Different pH

The absorption and fluorescence maxima of 2,5-dimethylphenol (25DMP) (1×10^{-4} M) in pH ~2, pH ~7, and pH ~11 buffer solutions containing different concentrations of α-CD and β-CD are presented in Table 1, Figure 1, and Figure 2. Since 25DMP exists predominantly as a monoanion at pH ~7, its inclusion behavior with CDs was examined in acidic, neutral, and alkaline media to evaluate both the neutral and monoanionic forms. In water and CD-containing solutions, the absorption and emission spectral profiles of 25DMP at pH ~2 and pH ~7 are nearly identical; however, noticeable differences appear at pH ~11. In CD-free aqueous solutions, the absorption maxima of 25DMP occur at 275–271 nm at pH ~2 and pH ~7, while at pH ~11 the maxima shift to 292–282 and 239 nm. Increasing α-CD or β-CD concentration produces no significant absorption shift at pH ~2 and pH ~7, although a shoulder develops at 292 nm in alkaline medium. In all three pH conditions, the absorbance slightly increases upon CD addition. The differences in absorption maxima and band shapes across the three pH values indicate the formation of distinct types of inclusion complexes in α-CD and β-CD.

The influence of β-CD on the fluorescence properties of 25DMP is more pronounced compared to α-CD. In CD-free solutions, the emission maxima at pH ~2 and pH ~7 are similar, whereas at pH ~11 the fluorescence profile differs. In α-CD, the emission maximum is observed at 305 nm in pH ~2 and pH ~7, shifting to 309 nm at pH ~11. With increasing α-CD concentration, the emission intensity decreases at pH ~2,

while at pH ~7 the intensity decreases along with a red shift from 305 to 311 nm; at pH ~11 the band shifts from 309 to 312 nm. For β-CD, increasing concentration leads to decreased emission intensity in all three pH values, accompanied by red shifts from 304 to 312 nm (pH ~2 and pH ~7) and 308 to 312 nm (pH ~11).

The presence of isosbestic points in the absorption spectra for all pH conditions supports the formation of 1: 1 inclusion complex between 25DMP and the CDs [4-16]. However, the differences observed between the spectra at pH ~2/pH ~7 relative to pH ~11 suggest the coexistence of at least two different types of inclusion complexes. Binding constants for the complexes were obtained using the Benesi–Hildebrand method. The negative values of ΔG (Table 1) confirm that inclusion is a spontaneous, exothermic process occurring readily at 303 K.

Table 1. *Absorption and fluorescence maxima of 2,5-dimethyl phenol (25DMP) with different α-CD and β-CD concentrations.*

Concentration of CD x10^{-3} M	**pH -3.0**				**pH - 7**				**pH - 11**			
	λ_{abs}	**log ε**	**λ_{flu}**	**τ**	**λ_{abs}**	**log ε**	**λ_{flu}**	**τ**	**λ_{abs}**	**log ε**	**λ_{flu}**	**τ**
25DMP only (without CD)	275	3.51	304	0.32	275	3.58	305	0.34	292 279 238	3.51	309	0.25
0.2 M α-CD	274	3.54	303	0.46	275	3.59	305	0.49	290 279 238	3.55	310	0.44
1.0 M α-CD	274	3.57	305	0.56	275	3.61	311	0.62	292-281 239	3.59	312	0.56
0.2 M β-CD	275	3.57 4.01	305	0.50	274	3.57	305	0.54	292-282 237 219	3.55	311	0.48
1.0 M β-CD	275 220	3.57 4.09	311	0.61	275 220	3.75	312	0.67	292-282 233 220	3.59	312	0.64
K (1: 1) x10^5 M^{-1} α-CD	46		900		20		420		16		240	
ΔG (kcalmol^{-1}) α-CD	-9.6		-17.1		-7.5		-15.2		-6.9		-13.8	
K (1: 1) x10^5 M^{-1} β-CD	40		130		12		128		41		370	
ΔG (kcalmol^{-1}) β-CD	-9.2		-12.2		-6.2		-12.2		-9.3		-14.8	
Excitation wavelength (nm)			270				270				270	

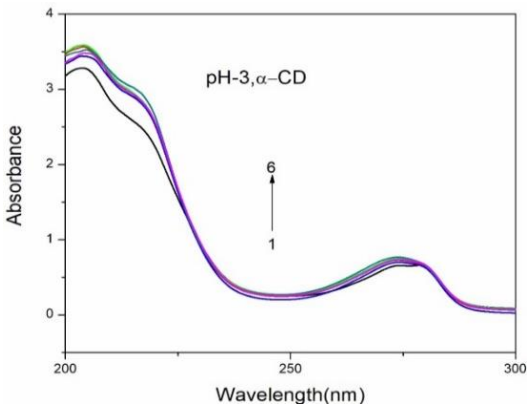

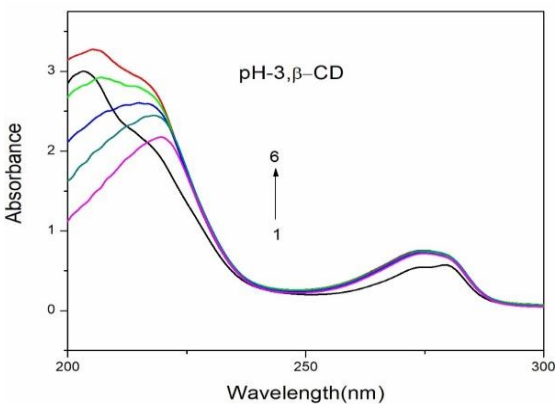

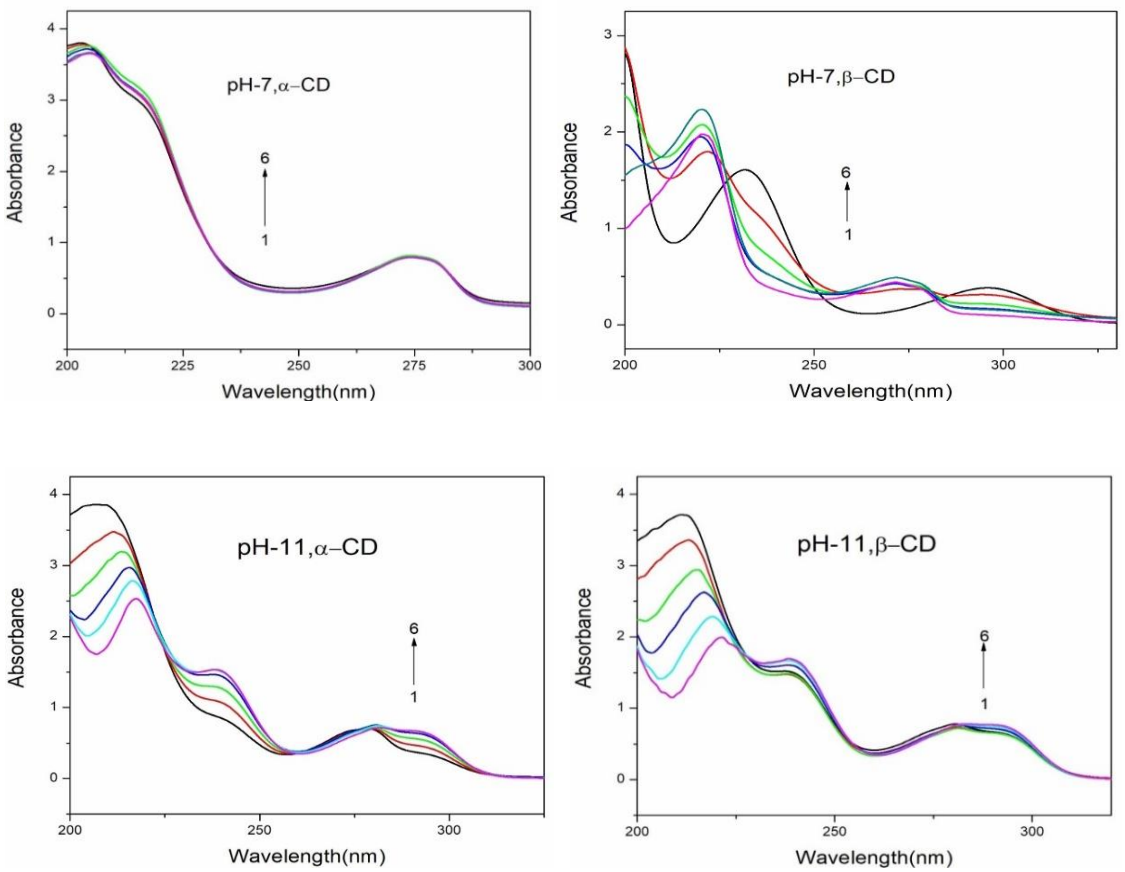

Figure 1. *Absorption spectra of 25DMP in different α-CD and β-CD concentrations (M): (1) 0, (2) 0.002, (3) 0.004, (4) 0.006, (5) 0.008 and (6) 0.01.*

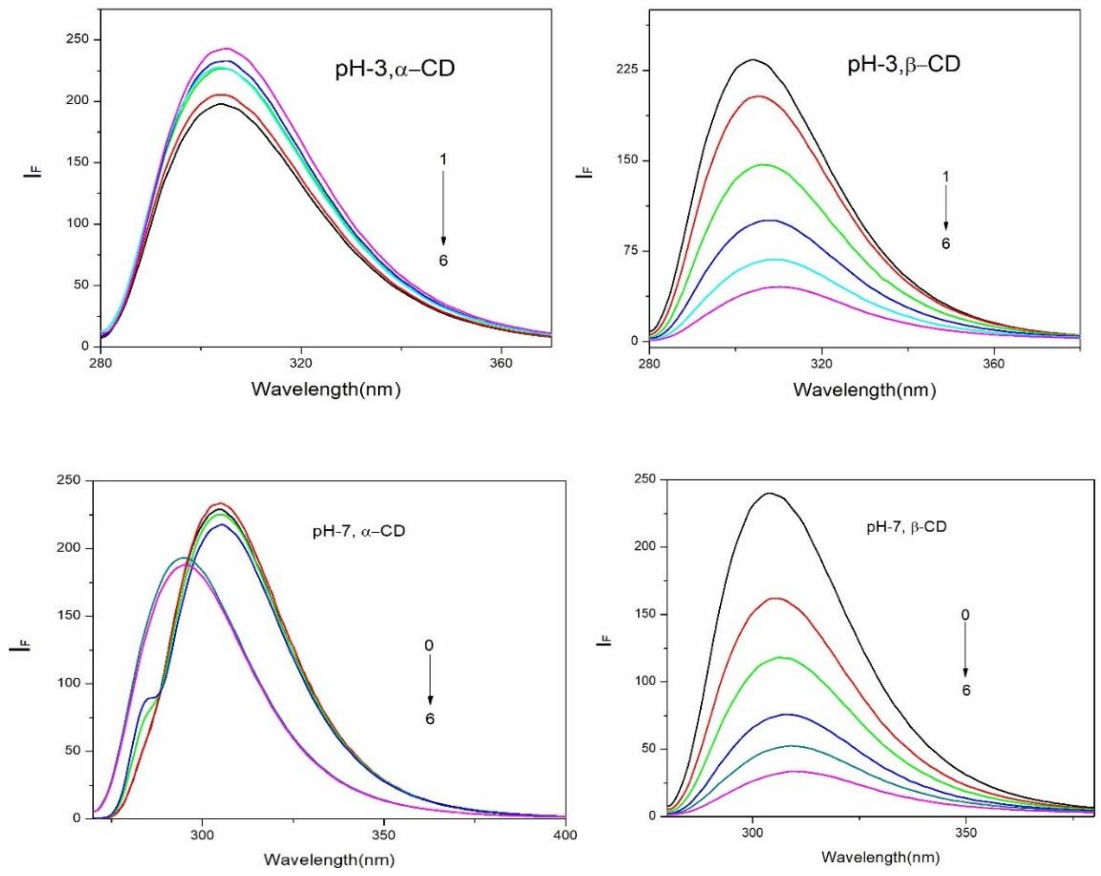

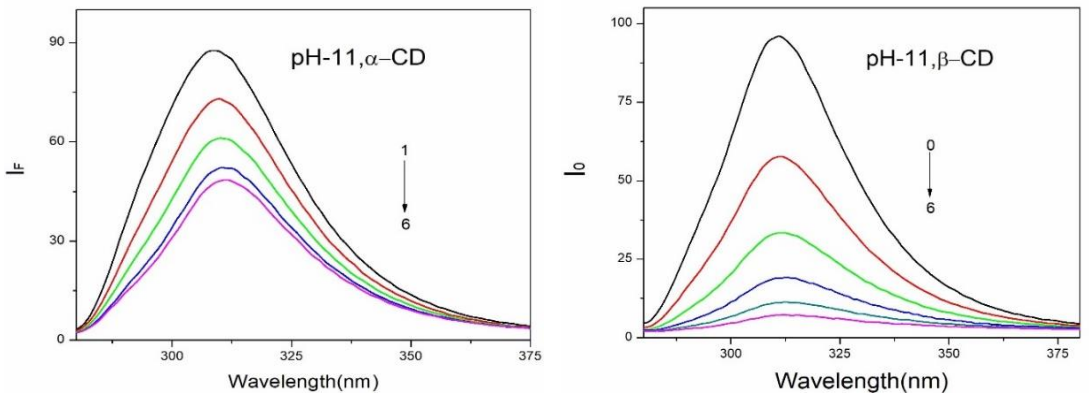

Figure 2. *Fluorescence spectra of 25DMP in different α-CD and β-CD concentrations (M): (1) 0, (2) 0.002, (3) 0.004, (4) 0.006, (5) 0.008 and (6) 0.01.*

Generally, the inclusion of guest molecules within cyclodextrin cavities is influenced by both hydrophobic and electronic interactions [4-16]. To further verify the inclusion process, the spectroscopic properties of 25DMP were compared with those recorded in various solvents (cyclohexane: λ_{abs} ~ 276 nm, λ_{emi} ~ 302 nm; acetonitrile: λ_{abs} ~ 276 nm, λ_{emi} ~ 303 nm; methanol: λ_{abs} ~ 275 nm, λ_{emi} ~ 305 nm; water (pH~3): λ_{abs} ~ 275 nm, λ_{emi} ~ 305 nm). Relative to phenol, 25DMP exhibits red-shifted absorption and emission maxima in all solvents [4] (phenol: cyclohexane: λ_{abs} ~ 271-277, 264 nm, λ_{emi} ~ 300 nm; acetonitrile: λ_{abs} ~ 272-278 nm, λ_{emi} ~ 305 nm; methanol: λ_{abs} ~ 273 nm, λ_{emi} ~ 305 nm; water (pH~2) ≈ λ_{abs} ~ 269 nm, λ_{emi} ~ 305 nm). Solvatochromic analysis shows that 25DMP does not undergo significant absorption or emission shifts from cyclohexane to water, with only a slight red shift in fluorescence noted when moving from nonpolar to polar media. The spectral behavior in protic and aprotic solvents aligns with the typical characteristics of hydroxyl-containing aromatic systems [4-16].

The absorption spectra of 25DMP in CD solutions closely resemble those of phenol, indicating that methyl substitution does not significantly alter the benzene ring conjugation. The broad absorption bands in both phenol and 25DMP suggest the presence of intermolecular hydrogen bonding. Across all pH conditions, increasing α-CD concentration results in increased absorbance and decreased fluorescence intensity. In β-CD solutions, absorbance increases at the same wavelength for all pH values, while the emission maximum consistently red shifts. Remarkably, at higher β-CD concentrations, the emission maximum converges to a single value (312 nm) in all pH conditions, and the absorption/emission profiles become identical—indicating the formation of a similar inclusion complex. In contrast, α-CD produces different emission maxima, implying a different mode of encapsulation.

These observations support that 25DMP forms distinct types of inclusion complexes with α-CD and β-CD. The molecule is more deeply encapsulated within the larger β-CD cavity, whereas only partial insertion occurs in α-CD. Although both CDs have the same height (7.8 Å), α-CD possesses a smaller interior cavity (4.7–5.3 Å) than β-CD (6.0–6.5 Å). Reduced dipole–dipole interactions within the less polar, hydrophobic cavity account for the observed increase in absorbance and decrease in emission intensity [4-16]. The red shift observed in the alkaline medium (pH ~11) is consistent with deprotonation of the phenolic –OH group. Notably, at high CD concentrations, the absorption and emission maxima and overall spectral shapes in pH ~1 and pH ~7 solutions become identical, confirming the formation of similar inclusion complexes. The high binding (formation) constants further indicate that 25DMP is strongly embedded within the CD cavities. Differences in cavity size and guest–host interactions between α-CD and β-CD account for the variations in association constants.

It has been previously reported that when carboxyl or hydroxyl groups are deeply embedded within the cyclodextrin cavity, the absorption and emission maxima undergo red or blue shifts, respectively, relative to aqueous solutions, because the interior of the CD cavity provides a nonpolar environment similar to cyclohexane [4-16]. Moreover, if the hydroxyl anion resides near the hydrophilic rim of the CD cavity, protonation may occur. In such cases, a blue shift is expected, and the spectral maxima should resemble those observed at pH ~3 or pH ~7, where the neutral form of the molecule predominates. The results in Table 1 show that the spectral maxima of the monoanionic form of 25DMP are similar to those in α-CD, whereas a blue shift is observed in β-CD. These observations confirm that, in 25DMP, the hydroxyl group is located in the nonpolar interior of the β-CD cavity, while in α-CD it remains closer to the hydrophilic exterior.

3.2. Excited Singlet State Lifetimes

The excited-state lifetimes of 25DMP in aqueous solution and in CD media, obtained from fluorescence decay curves, are listed in Table 1. The lifetimes of the inclusion complexes are greater than that of free 25DMP, likely due to restricted vibrational motion of the molecule within the CD cavity. Increasing CD concentration further enhances the lifetime, reflecting greater encapsulation. The longer lifetime of the

25DMP: β-CD complex compared with the 25DMP: α-CD complex indicates deeper penetration of the guest molecule into the β-CD cavity. These results demonstrate the stronger complexation ability and superior encapsulation efficiency of β-CD.

3.3. Molecular Modeling

The ground-state geometries of 25DMP and the CDs were optimized using the PM3 method (Table 2; Figure 3). In 25DMP, the vertical and horizontal distances between the –OH and $–CH_3$ groups are 5.72 Å and 6.77 Å, respectively (Figure 3). Both CDs possess a cavity height of 7.8 Å, with interior cavity diameters of 4.7–5.3 Å for α-CD and 6.0–6.5 Å for β-CD. The vertical dimension of 25DMP is smaller than the interior diameters of both CDs, whereas the horizontal dimension exceeds the cavity sizes. Thus, the distance between the two methyl substituents is greater than the CD interior diameter, suggesting that 25DMP can only be partially accommodated within the cavities.

These structural considerations confirm that the encapsulation mode in α-CD differs from that in β-CD. Because the vertical dimension of 25DMP is smaller than the upper rim of both CDs, the hydroxyl and methyl groups are positioned inside the β-CD cavity. However, due to its smaller cavity size, α-CD can encapsulate 25DMP only partially. These findings confirm the embedding of 25DMP within the CD cavities. The HOMO–LUMO energies, dipole moments, total energies, free energies, enthalpies, entropies, and zero-point vibrational energies of pure 25DMP, α-CD, and β-CD differ significantly from those of the inclusion complexes. Mulliken charge calculations indicate zero charge transfer between the host and guest, confirming that interactions are non-covalent. The thermodynamic parameters (ΔE, ΔG, and ΔH) further show that the formation of 25DMP–CD complexes is energetically favorable and driven predominantly by enthalpic contributions [4-16].

Table 2. *Thermodynamic parameters and HOMO-LUMO energy calculations for 25DMP and its inclusion complexes by PM6 method.*

Properties	25DMP	α-CD	β-CD	25DMP: α-CD	25DMP: β-CD
E_{HOMO} (eV)	-8.76	-10.37	-10.35	-8.51	-8.62
E_{LUMO} (eV)	0.38	1.26	1.23	0.49	0.53
$E_{HOMO} – E_{LUMO}$ (eV)	-9.15	-11.63	-11.58	-9.00	-9.15
Dipole moment (D)	1.33	11.34	12.29	11.58	11.69
E*	39.28	-1247.62	-1457.63	-1325.09	-1498.26
ΔE*	_	_	_	-116.74	-79.91
G*	70.19	-676.37	-789.52	637.27	739.71
ΔG*	_	_	_	-29.37	-20.38
H*	97.37	-570.84	-667.55	629.38	745.43
ΔH	_	_	_	-55.53	-62.25
S**	0.091	0.353	0.409	0.397	0.423
ΔS**	_	_	_	-0.047	-0.077
ZPE*		635.09	740.56	761.73	867.14
Mullikan charge	0.00	0.00	0.00	0.00	0.00

*kcal/mol; **kcal/mol-Kelvin; ZPE = Zero point vibration energy

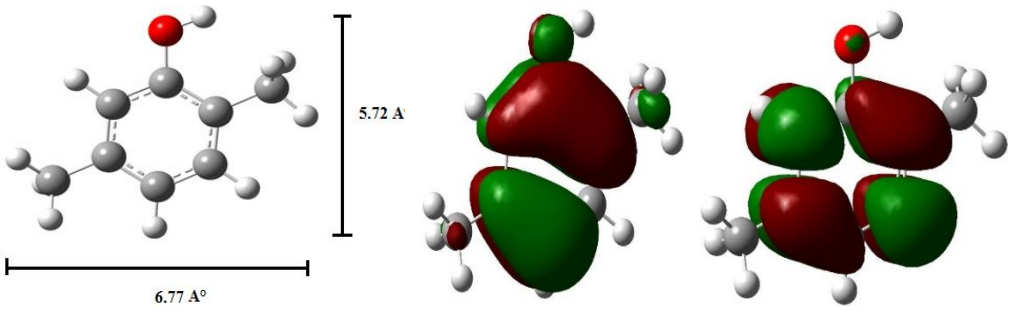

Figure 3. *PM3 optimized structures of (a, b) 25DMP, (c, d) HOMO, LUMO of 25DMP.*

3.4. Nanomaterial Studies

3.4.1. Scanning Electron Microscopy

The powdered forms of Cu nanoparticles, 25DMP, and the Cu: 25DMP: α-CD and Cu: 25DMP: β-CD inclusion complexes were examined using SEM (Figure 4). The images clearly show that copper nanoparticles appear as clustered spherical aggregates, while 25DMP exhibits an irregular stone-like morphology. In contrast, nanorod-type structures are observed in the Cu: 25DMP: α-CD and Cu: 25DMP: β-CD nanomaterials. SEM-EDX analysis confirms the presence of 49.95% carbon, 44.03% oxygen, and 3.98% copper in these nanomaterials. The modification in morphology compared to pure components supports the successful formation of the Cu: 25DMP: CD nanomaterials.

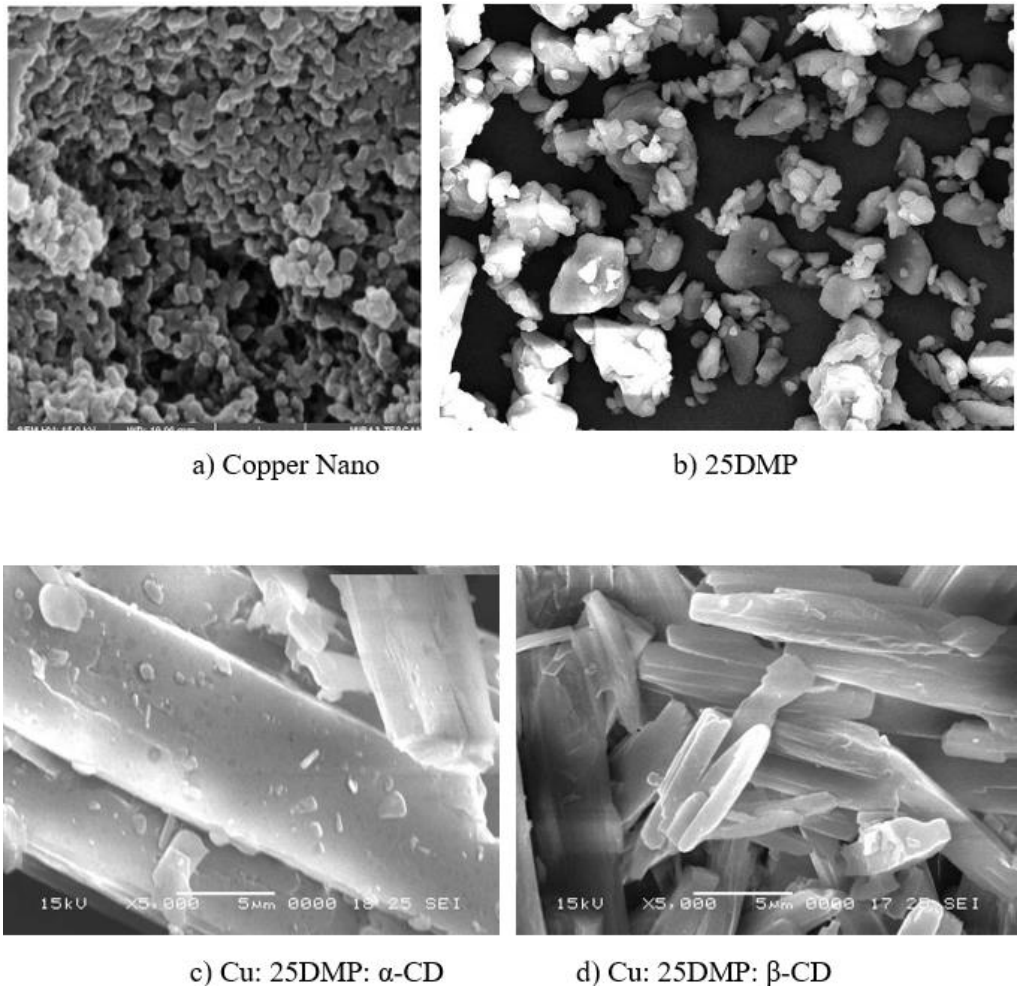

Figure 4. *SEM images of (a) 25DMP, (b) Cu: 25DMP: α-CD, (b) Cu: 25DMP: β-CD nano.*

3.4.2. Differential Scanning Colorimeter

The DSC profiles of 25DMP, α-CD, β-CD, and their inclusion complexes were recorded. The DSC curve of α-CD displays three endothermic peaks at 79.2°C, 109.1°C, and 137.5°C, while β-CD shows a broad endothermic peak at 128.6°C; these peaks correspond to the loss of crystal water [38-47]. The thermal curve of 25DMP exhibits a sharp endothermic peak at 77°C, corresponding to its melting point. The DSC curves of α-CD, β-CD, and their complexes show broader endothermic features due to water loss from the CDs. Notably, the DSC thermograms of the 25DMP: CD complexes do not display the characteristic peaks of pure 25DMP or CDs; instead, new peaks appear at 205°C for 25DMP: α-CD and 231°C for 25DMP: β-CD, indicating the formation of new inclusion complexes.

3.4.3. Infrared Spectral Studies

FTIR spectra of 25DMP, α-CD, β-CD, and the Cu: 25DMP: CD nanomaterials were also recorded. In 25DMP, the O–H stretching band appears at 3365 cm^{-1}, and the O–H out-of-plane vibration occurs at 709 cm^{-1}. Aromatic C–H, C–C, and C=C stretching vibrations are observed at 3046 cm^{-1}, 1589 cm^{-1}, and 1689 cm^{-1}, respectively. The C–CH_3 stretching region appears between 2976–2861 cm^{-1}, while CH_3 deformation bands are found at 1386 and 1425 cm^{-1}. C–H bending vibrations are noted at 768 and 807 cm^{-1}.

In the Cu: 25DMP: CD nanomaterials, the O–H stretching band shifts to 3260 cm^{-1}, while the aromatic C–H and C=C stretching bands shift to 2915 cm^{-1} and 1641 cm^{-1}, respectively. The C–O stretching bands observed at 1347 and 1039 cm^{-1} in 25DMP shift to 1337 and 1024 cm^{-1} in the nanomaterials. The Ar–O–H vibration, originally at 587 and 580 cm^{-1}, shifts to 573 cm^{-1}. Many characteristic 25DMP bands diminish or disappear in the nanomaterials, along with a significant decrease in intensity, indicating strong interactions between 25DMP, copper nanoparticles, and cyclodextrin.

3.4.4. XRD Spectral Studies

The crystallinity of all nanoparticles was evaluated using XRD analysis [38-47]. Pure copper nanoparticles exhibit distinct diffraction peaks at 43.31°, 50.44°, and 74.20°, which correspond to the characteristic reflections of a face-centered cubic (fcc) metallic copper lattice. The XRD pattern of α-CD shows crystalline peaks at approximately 11.94°, 14.11°, and 21.77°, while β-CD displays peaks at 11.49° and 17.58°. The intensity and visibility of these reflections may vary depending on sample conditions and preparation methods. The diffraction pattern of 25DMP, which crystallizes in the orthorhombic system, shows characteristic peaks at 7.33°, 10.51°, 21.15°, and 93.74°. In the Cu/25DMP: β-CD nanomaterial, new and well-defined diffraction peaks appear at 10.13°, 17.26°, 25.25°, 30.76°, 34.63°, 43.86°, 61.04°, and 72.75°. The differences in peak positions and intensities between the nanomaterials and their individual components confirm the formation of new composite nanostructures.

3.4.5. Proton Magnetic Resonance Spectral Studies

Table 3. ^{1}H-NMR chemical shift values for the 25DMP and Cu: 25DMP: CD nanomaterials.

Protons	25DMP (δ)	Cu: 25DMP: α-CD	Cu: 25DMP: β-CD
H_a - Para to OH	9.10	5.69	5.72
H_b - ortho to OH	6.90	4.78	4.83
H_c - meta to OH	6.52	4.48	4.51
H_d – OH	6.48	2.50	2.52
H_e - ortho CH_3	2.51	2.04	2.09
H_f - meta CH_3	2.11	1.25	1.26

^{1}H NMR spectroscopy is a valuable technique for probing structural features and host–guest interactions in cyclodextrin inclusion complexes. The proton assignments of CDs are well established; among them, H-3 and H-5 protons reside within the CD cavity, making their chemical shifts highly sensitive to guest inclusion. Conversely, H-1, H-2, and H-4 protons, located on the exterior, typically show only minor chemical shift variations. ^{1}H NMR spectra of free 25DMP and its inclusion complexes were recorded at 25°C in DMSO-d_6 (Table 3). The chemical shifts of the inclusion complexes differ markedly from those of the unbound molecule. Notably, the aromatic protons of the Cu: 25DMP: CD complexes shift upfield relative to free 25DMP, indicating their interaction with the inner cavity protons of the CDs. The increased chemical shift of the

hydroxyl proton of 25DMP suggests possible hydrogen bonding with CD hydroxyl groups. Additionally, the aromatic protons experience a greater upfield shift than the methyl protons in the complex, implying that the aromatic ring is strongly shielded within the Cu: 25DMP: CD nanomaterial. These observations collectively indicate that 25DMP penetrates deeply into the copper–CD cavity environment.

4. Conclusion

The absorption, emission, and time-resolved fluorescence maxima of 2,5-dimethylphenol (25DMP) were examined in various solvents as well as in α-CD and β-CD at pH ~2, pH ~7, and pH ~11. Nanomaterials were synthesized and characterized using SEM, DSC, FTIR, XRD, and ^{1}H NMR techniques. At pH ~2 and pH ~7, the absorption and emission maxima and the overall spectral profiles of 25DMP in α-CD and β-CD solutions are similar, whereas significant differences observed at pH ~11 indicate the presence of at least two distinct types of inclusion complexes. PM3 calculations suggest that 25DMP is more deeply encapsulated within the hydrophobic cavity of β-CD than in α-CD. Solvatochromic analysis shows no appreciable shift in the absorption or emission maxima of 25DMP from cyclohexane to water, indicating minimal solvent polarity effects. The fluorescence lifetimes of the 25DMP: CD inclusion complexes were longer than those of free 25DMP, consistent with restricted molecular motion upon encapsulation. SEM, DSC, FTIR, XRD, and ^{1}H NMR results clearly differentiate pure Cu nanoparticles, free 25DMP, and the Cu: 25DMP: α-CD and Cu: 25DMP: β-CD nanomaterials, confirming successful formation of the complexes. SEM-EDX analysis further verifies the composition of the nanomaterials, showing 49.95% carbon, 44.03% oxygen, and 3.98% copper.

Abbreviations

FTIR	Fourier Transform Infrared Spectroscopy
DTA	Differential Thermal Analysis
XRD	X-ray Diffraction
SEM	Scanning Electron Microscopy
HOMO	Highest Occupied Molecular Orbital
LUMO	Lowest Unoccupied Molecular Orbital
25DMP	2,5-dimethylphenol
Ag NPs	Silver Nanoparticles
α-CD	Alpha Cyclodextrin
β-CD	Beta Cyclodextrin
PM3	Parametric Method 3
ΔE	Iinternal Energy Change
ΔH	Enthalpy Change
ΔG	Free Energy Change
ΔS	Entropy Change

Author Contributions

Narayanasamy Rajendiran: Supervision, Resources, Methodology, Software, Writing – original draft, Writing – review & editing

Ayyadurai Mani: Formal Analysis, Investigation

Palanichamy Ramasamy: Data curation

Sengamalai Senthilmurugan: Validation

Conflicts of Interest

The authors declare no conflict of interest.

References

[1] H. H. Jaffe, M. Orchin, Theory and Applications of Ultraviolet Spec troscopy, Wiley, New York, 1962.

[2] J. F. Ireland, P. A. H. Wyatt, Adv. *Acid-base properties of electronically excited states of organic molecules*, Phys. Org. Chem. 12(1976) 132-215.

[3] S. J. Formosinho, L. G. Arnaut, *Excited-state proton transfer reactions I. Fundamentals and intermolecular reactions*, J. Photochem. Photobiol. A: Chem. 75(1993) 1. https://doi.org/10.1016/1010-6030(93)80002-4

[4] T. Stalin, R. Anithadevi, N. Rajendiran, Spectral characteristics of ortho, meta and para-dihydroxybenzenes in different solvents, pH and β-CD. *Spectrochimica Acta,* 61A(2005) 2495-2504. https://doi.org/10.1016/j.saa.2004.08.024

[5] T. Stalin, P. Vasantharani, B. Shanthi, A. Sekar, N. Rajendiran, Inclusion complex of 1,2,3-trihydroxy benzene with α- and β-cyclodextrins. *Indian J Chemistry*, 45A(2006) 1113-1120.

[6] R. K. Sankaranarayanan, S. Siva, A. Antony Muthu Prabhu, N. Rajendiran, A study on the inclusion complexation of 3,4,5-trihydroxy benzoic acid with β-CD at different pH. *J. Inclusion Phenomena and Macrocyclic Chemistry*, 67(2010) 461-470. https://doi.org/10.1007/s10847-009-9729-0

[7] M. Jude Jenita, J. Saravanan, N. Rajendiran, Inclusion complexation of dihydroxy benzene derivatives with α- and β-CDs. *J. Indian Chemical Society,* 91 May (2014) 899-911,

[8] S. Siva, R. K. Sankaranarayanan, A. Antony Muthu Prabhu, N. Rajendiran, Inclusion complexation of 3,5-dihydroxy benzoic acid with β-CD at different pH. Indian J. Chemistry, 48A (2009)1515-1521.

[9] T. Stalin, G. Sivakumar, B. Shanthi, A. Sekar, N. Rajendiran, Photophysical behaviour of 4-hydroxy-3,5-dimethoxy benzoic acid in different solvents, pH and β-cyclodextrin. *J. Photochem. Photobiol. A: Chemistry*, 177(2006) 144-155, https://doi.org/10.1016/j.jphotochem.2005.06.021

[10] T. Stalin, N. Rajendiran, A study on the spectroscopy and photophysics of 4-hydroxy-3-methoxy benzoic acid in different solvents, pH and β-cyclodextrin. *J. Molecular Structure*, 794(2006) 35-45, https://doi.org/10.1016/j.molstruc.2005.10.030

[11] N. Rajendiran, N. Ratha, M. Swaminathan, Solvatochromism and proton transfer kinetics of 1,5 and 1,7-naphthalenediols in the excited singlet state: A study by electronic spectra. *Indian J. Chemistry*, 40A(2001) 331-339.

[12] A. Antony Muthu Prabhu, G. Venkatesh, N. Rajendiran, Azo-Hydrazo tautomerism in 1-phenyazo-2-naphthol dyes in various solvents, pH and β-CD, *J. Fluorescence*, 20(2010) 961-972. https://doi.org/10.1007/s10895-010-0647-4

[13] J. Prema Kumari, A. Antony Muthu Prabhu, G. Venkatesh, V. K. Subramanian, N. Rajendiran, Effect of solvents and pH on β-CD Inclusion complexation of 2,4-dihydroxy azobenzene and 4-hydroxy azobenzene. *J.Solution Chemistry*, 40(2011) 327-347, https://doi.org/10.1007/s10953-010-9715-4

[14] A. Antony Muthu Prabhu, V. K. Subramanian, N. Rajendiran, Excimer formation in inclusion complexes of β-CD with salbutamol, sotalol and atenolol: Spectral and molecular modeling studies. *Spectrochimica Acta*, 96A(2012) 95-107, https://doi.org/10.1016/j.saa.2012.05.060

[15] M. Jude Jenita, T. Mohandoss, N. Rajendiran, Spectral and molecular modeling studies on hydroxy benzaldehydes with native and modified cyclodextrins. *J. Fluorescence,* 24(2014) 695-707, https://doi.org/10.1007/s10895-013-1352-3

[16] N. Rajendiran, G. Venkatesh, Inclusion complexation of 4,4'-dihydroxy benzophenone and 4-hydroxy benzophenone with α- and β-CD. *Supramolecular Chemistry*, 26(2014) 783-795, https://doi.org/10.1080/10610278.2014.940911

[17] R. Manoharan, S. K. Dogra, *Spectral characteristics of phenylenediamines and their various protonated species*, Bull. Chem. Soc. Jpn. 60 (1987) 4401. https://doi.org/10.1246/bcsj.60.4401

[18] R. Manoharan, S. K. Dogra, *Acidity constants in the excited states: absence of an excited-state prototropic equilibrium for the monocation-neutral pair of 2,3-diaminonaphthalene*, J. Phys. Chem. 92(1988) 5282. https://doi.org/10.1021/j100329a046

[19] A. Paul, R. S. Sarpal, S. K. Dogra, *Effects of solvent and acid concentration on the absorption and fluorescence spectra of α,α-diaminonaphthalenes*, J. Chem. Soc., Faraday Trans. I 86(1990) 2095. https://doi.org/10.1039/FT9908602095

[20] J. R. Lakowictz, Principles of Fluorescence Spectroscopy, Kluwer Academic Publishers/Plenum Press, New York, 1999.

[21] S. Akkın, G. Varan, D. Aksüt, M. Malanga, A. Ercan, M. Şen, et al., A different approach to immunochemotherapy for colon cancer: Development of nanoplexes of cyclodextrins and interleukin-2 loaded with 5-FU, *Int. J. Pharm.* 623(2022) 121940. https://doi.org/10.1016/j.ijpharm.2022.121940.

[22] N. A. Alhakamy, S. M. Badr-Eldin, O. A. A. Ahmed, H. M. Aldawsari, S. Z. Okbazghi, M. A. Alfaleh, et al., Green nanoemulsion stabilized by in situ self-assembled natural oil/native cyclodextrin complexes: An eco-friendly approach for enhancing anticancer activity of costunolide against lung cancer cells, *Pharmaceutics* 14(2022) 227. https://doi.org/10.3390/pharmaceutics14020227

[23] K. Zheng, X. Liu, H. Liu, D. Dong, L. Li, L. Jiang, et al., Novel pH-triggered doxorubicin-releasing nanoparticles self-assembled by functionalized β-cyclodextrin and amphiphilic phthalocyanine for anticancer therapy, *ACS Appl. Mater. Interfaces* 13(2021) 10674-10688. https://doi.org/10.1021/acsami.0c19027

[24] Y. Zhang, X. Li, X. Chen, Y. Zhang, Y. Deng, Y. Yu, et al., Construction of ultrasmall gold nanoparticles based contrast agent via host-guest interaction for tumor-targeted magnetic resonance imaging, *Mater. Des.* 217(2022) 110620. https://doi.org/10.1016/j.matdes.2022.110620

[25] R. Zhang, X. You, M. Luo, X. Zhang, Y. Fang, H. Huang, et al., Poly(β-cyclodextrin)/platinum prodrug supramolecular nano system for enhanced cancer therapy: Synthesis and in vivo study, *Carbohydr. Polym.* 292(2022) 119695. https://doi.org/10.1016/j.carbpol.2022.119695

[26] Y. Yuan, T. Nie, Y. Fang, X. You, H. Huang, J. Wu, Stimuli-responsive cyclodextrin-based supramolecular assemblies as drug carriers, *J. Mater. Chem. B* 10(2022) 2077-2096. https://doi.org/10.1039/d1tb02683f

[27] H. M. Ameen, S. Kunsági-Máté, L. Szente, B. Lemli, Encapsulation of sulfamethazine by native and randomly methylated β-cyclodextrins: The role of the dipole properties of guests. *Spectrochim. Acta A* 225(2020) 117475. https://doi.org/10.1016/j.saa.2019.117475

[28] M. Jamrógiewicz, K. Milewska, Sacharides and their derivatives as pharmaceutical additives *Spectrochim. Acta A* 219 (2019) 346. https://doi.org/10.1016/j.saa.2019.03.040

[29] M. A. Chouker, H. Abdallah, A. Zeiz, M. H. El-Dakdouki, Host-guest inclusion complex of quinoxaline-1,4-dioxide derivative with 2-hydroxypropyl-β-cyclodextrin: Preparation, characterization, and antibacterial activity. *J. Mol. Struct.* (2021) 130273. https://doi.org/10.1016/j.molstruc.2021.130273

[30] M. Levine, B. R. Smith, Tuning fluorescence energy transfer for carcinogen detection and medical diagnostics. *J. Fluoresc.* 30 (2020) 1015. https://doi.org/10.1007/s10895-020-02577-1

[31] S. K. Dogra, Proc. Inter- and intramolecular proton transfer reactions in 2-(2′-aminophenyl)-1H-imidazole, Indian Acad. Sci. 104 (1992) 635.

[32] N. Rajendiran, M. Swaminathan, Excited sate proton transfer kinetics of 4-hydroxy diphenyl ether. *International J. Chemical Kinetics*, 29 (1997) 861-867, https://doi.org/10.1002/(SICI)1097-4601(1997)29:11<861::AID-KIN8>3.0.CO;2-K

[33] A. Mani, P. Ramasamy, A. Antony Muthu Prabhu, N. Rajendiran, Investigation of Ag and Ag/Co bimetallic nanoparticles with naproxen-cyclodextrin inclusion complex. J. Molecular Structure, 1284(2023) 135301-10. https://doi.org/10.1016/j.molstruc.2023.135301

[34] A. Mani, G. Venkatesh, P. Senthilraja, N. Rajendiran, Synthesis and Characterisation of Ag-Co-Venlafaxine-Cyclodextrin Nanorods, European J Advanced Chemistry Research, 5(2024) 9-16. https://doi.org/10.24018/ejchem.2024.5.1.147

[35] A. Mani, P. Ramasamy, A. Antony Muthu Prabhu, P. Senthilraja, N. Rajendiran, Synthesis and Analysis of Ag/Olanzapine /Cyclodextrin and Ag/Co/Olanzapine /Cyclodextrin Inclusion Complex Nanorods. Physics and Chemistry of Liquids, 62(2024) 196-209. https://doi.org/10.1080/00319104.2023.2297223

[36] A. Mani, P. Ramasamy, A. Antony Muthu Prabhu, P. Senthilraja, N. Rajendiran, Synthesis and Characterisation of Ag/Co/Chloroquine/Cyclodextrin Inclusion Complex Nanomaterials. J Sol-Gel Science and Technology 115(2025) 844-856.https://doi.org/10.1007/s10971-024-06620-5.

[37] N. Rajendiran, A. Mani, M. Venkatesan, B. Sneha, E. Nivetha, P. Senthilraja, Spectral, Microscopic, Antibacterial and Anticancer Activity of Pyrimethamine drug with Ag nano, DNA, RNA, BSA, Dendrimer, and Cyclodextrins, J Solution Chem, In press. https://doi.org/10.1007/s10953-025-01529-1

[38] P Ramasamy, A Mani, B Sneha, E Nivetha, M Venkatesan, N Rajendiran, Azo-hydrazo tautomerism in Sudan Red-B and Cyclodextrin/ Sudan Red-B doped ZnO nanomaterials. J Molecular Structure 1329(2025) 141423-32. https://doi.org/10.1016/j.molstruc.2025.141423

[39] P. Ramasamy, A. Mani, B. Sneha, E. Nivetha, A. Antony Muthu Prabhu, G. Venkatesh, N. Rajendiran,* Synthesis and Characterisation of Sudan Red-G/Cyclodextrin doped ZnO Nanocrystals. American J Physical Chemistry 14(2025) 23-32, https://doi.org/10.11648/j.ajpc.20251402.12

[40] P. Ramasamy, A. Mani, B. Sneha, E. Nivetha, A. Antony Muthu Prabhu, G. Venkatesh, P. Senthilraja, N. Rajendiran*, Synthesis and Characterisation of Cyclodextrin /Methyl Violet doped ZnO Nanocrystals. Colloid and Surface Science 9(2025) 19-30, https://doi.org/10.11648/j.css.20250701.12.

[41] P. Ramasamy, A. Mani, B. Sneha, E. Nivetha, A. Antony Muthu Prabhu, G. Venkatesh, P. Senthilraja, N. Rajendiran*, Synthesis and Characterisation of Cyclodextrin/ Sudan Black-B Caped ZnO/ Nanocrystals. American J Quantum Chemistry and Molecular Spectroscopy 9(2025) 1-11, https://doi.org/10.11648/j.ajqcms.20250901.11

[42] P. Ramasamy, A. Mani, A. Antony Muthu Prabhu, G. Venkatesh, N. Rajendiran* Azo-Imino Tautomerism in Sudan Red 7B/Cyclodextrin Coated ZnO Nanocomposites: Evidence by Spectral and Microscopic Perspectives. Science Journal of Chemistry 13(2025) 65 - 75, https://doi.org/10.11648/j.sjc.20251303.13

[43] P. Ramasamy, A. Mani, A. Antony Muthu Prabhu, G. Venkatesh, P. Senthilraja, N. Rajendiran* PICT Effects and Anticancer Potential on Rosaniline and Spectral Characterisation of Rosaniline/Cyclodextrin Covered ZnO/ Nanocrystals. International J. Pure and Applied Chemistry 26(2025) 107-121, https://doi.org/10.9734/irjpac/2025/v26i3921

[44] P. Ramasamy, A. Mani, P. Senthilraja, N. Rajendiran Keto-Enol Tautomerism and Anticancer Potential on Sudan Blue II and Synthesis and Characterisation of Sudan Blue II/ Cyclodextrin doped ZnO Nanocrystals, J. Materials Science and Nanotechnology, 13(2025) 1-16.

[45] P. Ramasamy, A. Mani, P. Senthilraja, N. Rajendiran, Spectral, Microscopic and Anticancer Activity Investigation on Dimethyl Yellow/Cyclodextrin Doped ZnO Nanocomposites Journal of Chemical and Pharmaceutical Sciences (JCHPS) 18(3) (2025) 33-43.

[46] P. Ramasamy, A. Mani, P. Senthilraja, N. Rajendiran, Spectral Characteristics of ZnO/Mordent Yellow 12/ Cyclodextrin Nanomaterials, J Chemical Health Risks, (JCHR) 15(2025) 542-553 www.jchr.org

[47] P. Ramasamy, A. Mani, P. Senthilraja, S. Senthilmurugan, N. Rajendiran, Spectral, Microscopic and Anticancer Activity of 1,8-Diaminonaphthalene Doped ZnO Nanocrystals, VVI-JOURNAL 14(2026) 135-147, https://vvijournal.com/